JOC The Journal of Organic Chemistry

ARTICLE

pubs.acs.org/joc

# Glucokinase-Activating Sesquinlignans from the Rhizomes of *Acorus tatarinowii* Schott

Gang Ni, Zhu-Fang Shen, Yang Lu, Ying-Hong Wang, Yan-Bo Tang, Ruo-Yun Chen, Zhi-You Hao, and De-Quan Yu*

The Key Laboratory of Bioactive Substances and Resources Utilization of Chinese Herbal Medicine, Peking Union Medical College, Ministry of Education, and Institute of Materia Medica, Chinese Academy of Medical Sciences and Peking Union Medical College, Beijing 100050, P. R. China

Supporting Information

**ABSTRACT:** Three novel sesquinlignans, tatanans A (**1**), B (**2**), and C (**3**), have been isolated from the rhizomes of *Acorus tatarinowii* Schott. Their structures were established by spectroscopic techniques and single-crystal X-ray analysis. Tatanans A−C potently increase GK enzymatic activity with $EC_{1.5}$ values in the range of 0.16−1.85 $\mu$M. The potent GK activity and unique structural features of tatanans make them promising leads for therapeutic development of antihyperglycemic drugs.

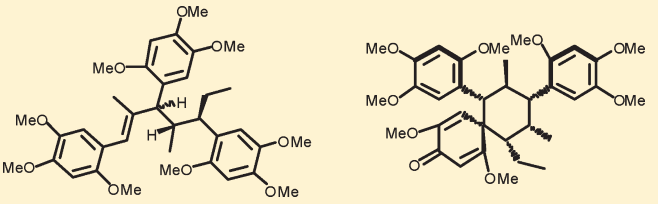


## INTRODUCTION

Type 2 diabetes mellitus (T2DM) is a polygenic disease affecting over 150 million people worldwide.[1] This disease is characterized by elevated blood glucose concentrations, insulin resistance, excessive hepatic glucose production, and reduced glucose-triggered insulin secretion.[2] Currently, no single marketed drug is capable of achieving enduring blood glucose control in the majority of T2DM patients.[3] Therefore, there remains a significant need for the development of new, safe, and effective therapeutic agents with novel and multiple modes of action. Glucokinase (GK), one of the four hexokinases, catalyzes the phosphorylation of glucose to glucose-6-phosphate. It plays a key role in whole-body glucose homeostasis by enhancing insulin secretion from pancreatic $\beta$-cells and glucose metabolism in the liver. GK activators (GKAs) have shown promising glucose-lowering effects in animal models of T2DM by increasing pancreatic insulin secretion and by augmenting hepatic glucose metabolism.[4−6] In fact, certain GKAs have advanced into human clinical studies.[7−9]

"Chang-Pu", a famous traditional Chinese medicine, has been used in the therapy of epilepsy and the improvement of memory and cognition.[10] This herb includes the rhizomes of three major *Acorus* (Araceae) species, *A. calamus* L., *A. gramineus* Soland, and *A. tatarinowii* Schott.[11] *Acorus calamus* L. is widely used for the treatment of diabetes in traditional folk medicine of America and Indonesia, and there are several reported cases where the root had cured people who had been deemed incurable by Western medicine.[12] The ethyl acetate fraction of *A. calamus* L. exhibited significant insulin-releasing and α-glucosidase inhibitory activities.[13] As part of our ongoing search for structurally and pharmacologically interesting metabolites from traditional Chinese medicine, we found that the ethyl acetate fraction of *A. tatarinowii* Schott also showed antihyperglycemic activity. Activity-guided isolation furnished tatanans A−C (**1**−**3**), three novel sesquinlignans with the unprecedented carbon skeleton as characterized by a unique C8−C7′ linkage pattern. Remarkably, tatanans A−C (**1**−**3**) potently increase GK enzymatic activity with $EC_{1.5}$ values in the range of 0.16−5.53 $\mu$M. The potent GK activity and unique structural features of tatanans make them promising leads for therapeutic development of a new generation of antihyperglycemic drugs. Furthermore, this is the first report on natural products with significant GK enzymatic activity. We report herein the isolation, structural elucidation, quantitative analysis, and antidiabetic bioactivities of tatanans A−C (**1**−**3**).

## RESULTS AND DISCUSSION

Tatanan A (**1**) was obtained as a white solid. Its molecular formula was determined to be $C_{36}H_{48}O_9$ by HREIMS at $m/z$ 624.3267 $[M]^+$ (calcd 624.3298). The UV spectrum exhibited absorption maxima at 204, 232 (sh), 259, and 296 nm. Its IR spectrum disclosed absorption bands assignable to the benzene ring (1606, 1509, and 1465 $cm^{-1}$) moiety. The $^1H$ NMR spectrum of **1** (Table 1) showed six aromatic hydrogens at $\delta$ 6.54 (2H, s, H-3″,6″), 6.59 (1H, s, H-3), 6.64 (1H, s, H-6), 6.66 (1H, s, H-3′), and 6.87 (1H, s, H-6′), which were ascribed to the hydrogens of three tetrasubstituted aromatic rings and nine methoxy groups that usually exists in lignans. Furthermore, three sets of methyl groups, three sets of $sp^3$ methine groups, one $sp^3$ methylene group, and an olefinic methine proton at $\delta$ 6.28 were observed in the $^1H$ NMR spectrum. The $^{13}C$ NMR spectrum (Table 1) revealed signals for 36 carbons: 13 quaternary carbons, 10 methines, one methlyene, and 12 methyls. These signals were assigned from the HSQC and COSY spectra. All proton signals

**Received:** November 16, 2010
**Published:** March 02, 2011

Table 1. $^{1}H$ and $^{13}C$ NMR Data ($\delta$) of Compounds 1−3

| | 1[a] | | 2[b] | | 3[b] | |
|---|---|---|---|---|---|---|
| no. | $\delta_H$ m (J, Hz) | $\delta_C$ | $\delta_H$ m (J, Hz) | $\delta_C$ | $\delta_H$ m (J, Hz) | $\delta_C$ |
| 1 | | 121.4 | | 119.9 | | 120.7 |
| 2 | | 153.5 | | 153.4 | | 153.7 |
| 3 | 6.59 (s) | 98.7 | 6.55 (s) | 99.2 | 6.49 (s) | 97.6 |
| 4 | | 149.8 | | 149.7 | | 149.8 |
| 5 | | 143.8 | | 143.1 | | 142.7 |
| 6 | 6.64 (s) | 116.6 | 6.51 (s) | 119.0 | 6.82 (s) | 114.7 |
| 7 | 6.28 (s) | 123.0 | 3.17 (d, 11.0) | 61.0 | 3.84 (d, 11.4) | 50.6 |
| 8 | | 139.7 | 3.45 (m) | 27.4 | 2.81 (m) | 30.3 |
| 9 | 1.57 (s) | 14.9 | 0.63 (d, 6.0) | 19.5 | 0.50 (d, 6.0) | 19.0 |
| 1′ | | 125.1 | | 124.0 | | 123.9 |
| 2′ | | 154.2 | | 153.3 | | 153.4 |
| 3′ | 6.66 (s) | 100.0 | 6.76 (s) | 99.6 | 6.72 (s) | 99.3 |
| 4′ | | 149.2 | | 149.6 | | 149.6 |
| 5′ | | 143.7 | | 143.7 | | 143.7 |
| 6′ | 6.87 (s) | 115.2 | 6.92 (s) | 117.1 | 6.95 (s) | 117.9 |
| 7′ | 3.53 (overlap) | 52.0 | 3.27 (dd, 12.0, 4.5) | 48.1 | 3.39 (dd, 12.0, 4.2) | 48.3 |
| 8′ | 2.56 (1H, m) | 38.3 | 2.32 (m) | 33.7 | 2.33 (m) | 33.4 |
| 9′ | 0.97 (d, 6.5) | 15.8 | 0.94 (d, 7.5) | 12.3 | 0.99 (d, 7.2) | 12.4 |
| 1″ | | 123.8 | | 56.3 | | 55.2 |
| 2″ | | 154.6 | | 177.5 | | 178.6 |
| 3″ | 6.54 (s) | 99.9 | 5.38 (s) | 105.8 | 5.22 (s) | 104.6 |
| 4″ | | 149.2 | | 181.3 | | 181.1 |
| 5″ | | 143.4 | | 151.0 | | 152.8 |
| 6″ | 6.54 (s) | 116.6 | 6.29 (s) | 116.3 | 6.27 (s) | 117.4 |
| 7″ | 3.11 (m) | 29.5 | 2.43 (dt, 11.0, 4.5) | 49.9 | 2.51 (dt, 11.4, 4.8) | 49.3 |
| 8″ | a 1.74 (m) b 1.80 (1H, m) | 27.2 | a 1.15 (m) b 1.24 (m) | 21.6 | a 1.13 (m) b 1.27 (m) | 21.9 |
| 9″ | 0.77 (t, 6.5) | 13.3 | 0.79 (t, 7.5) | 12.0 | 0.78 (t, 7.2) | 12.0 |
| OMe | 3.53 (s) | 56.1 | 3.67 (s) | 54.7 | 3.61 (s) | 55.0 |
| OMe | 3.71 (9H, overlap) | 56.7 | 3.72 (s) | 55.7 | 3.70 (6H, overlap) | 56.0 |
| OMe | 3.77 (s) | 56.8 | 3.77 (s) | 56.1 | 3.73 (overlap) | 56.1 |
| OMe | 3.78 (s) | 56.8 | 3.80 (s) | 56.1 | 3.74 (overlap) | 56.3 |
| OMe | 3.82 (s) | 56.9 | 3.86 (overlap) | 56.1 | 3.78 (s) | 56.5 |
| OMe | 3.84 (s) | 57.3 | 3.87 (overlap) | 56.9 | 3.83 (s) | 56.8 |
| OMe | 3.87 (s) | 57.6 | 3.88(overlap) | 57.0 | 3.86 (s) | 57.8 |
| OMe | | 57.6 | 3.89 (overlap) | 58.0 | | 58.4 |
| OMe | | 57.8 | | | | |

[a] In $CD_3OD$. [b] In acetone-$d_6$.

were unambiguously assigned to their respective carbon atoms by the HSQC data. Interpretation of the COSY and HSQC data of **1** indicated the presence of the C7′−C8′(C9′)−C7″−C8″−C9″ subunit (see Figure 2). Protons $H_3$-9 showed a weak $^{1}H-^{1}H$ long-range coupling to H-7. The subunit and nonprotonated carbons were connected to each other on the basis of HMBC correlations. In the HMBC spectrum, the long-range correlations from H-7 to C-1, C-2, C-6, C-8, and C-9, from H-6 to C-1, C-2, C-4, C-5, and C-7, and from H-3 to C-1, C-2, C-4, and C-5 confirmed the presence of a $C_6-C_3$ unit. Key HMBC correlations from H-7, H-9, and H-6′ to C-7′, from H-8′ to C-1″, and from H-6″ to C-7″ led to the construction of a novel sesquilignan with an unprecedented C8−C7′ linkage pattern of $C_6-C_3$ units (Figures 1 and 2).

Because **1** possesses such a unique, acyclic carbon skeleton, we could not assign its configuration with the NMR data. Thus, confirmation of the entire structure of **1** by single-crystal X-ray diffraction analysis was highly desirable. Recrystallization of **1** by slow evaporation from a mixture of $MeOH/H_2O$ furnished single crystals suitable for X-ray analysis. The performance of a single-crystal X-ray diffraction allowed the definite assignment of the structure of **1** (Figure 3). Cu Kα radiation was used in the single-crystal X-ray diffraction, and the value of the Flack parameter (0.0 (3)) allowed assignment of absolute configuration of all the stereogenic centers in **1** as 7′*S*8′*S*7″*R*. The geometry of the C-7/8 double bond was assigned as *E*.

Tatanan B (**2**) was isolated as white needles whose molecular formula of $C_{35}H_{46}O_9$ was established on the basis of HREIMS at *m*/*z* 610.3143 $[M]^+$ (calcd 610.3142). This molecular formula was 14 mass units less than that of **1**, suggesting the loss of methylene. Signals of three tetrasustituted aromatic rings (six singlets) remained after comparison of the $^{1}H$ NMR data of


dx.doi.org/10.1021/jo1022712 |J. Org. Chem. 2011, 76, 2056–2061

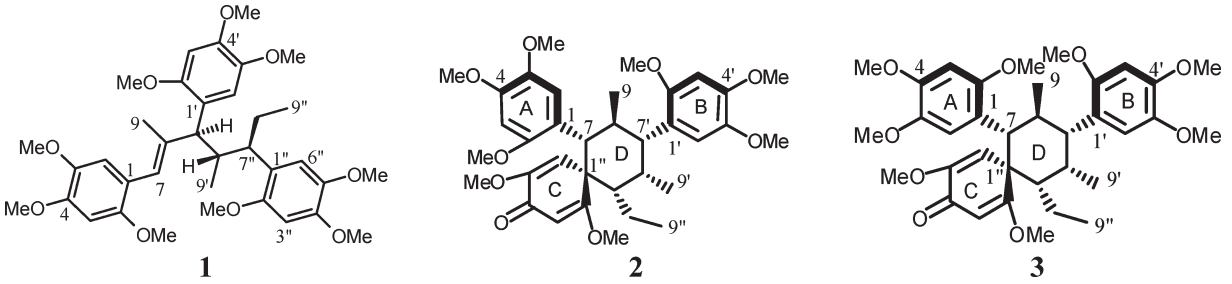

**Figure 1.** Structures of tatanans A−C (**1**−**3**).

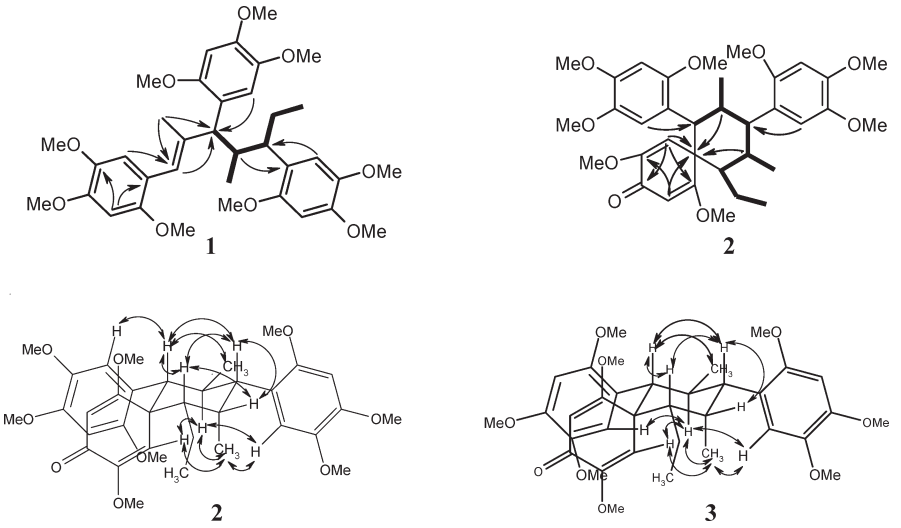

**Figure 2.** Selected COSY (bold bonds), HMBC (single-headed arrows), and NOESY (double-headed arrows) correlations of **1**−**3**.

**2** and **1** (Table 1). However, one of three aryl groups showed exceptional chemical shifts at $\delta$ 5.38 (H-3″) and 6.29 (H-6″). The corresponding shifts in the $^{13}$C NMR spectrum were also very different from those of the tetrasustituted aromatic ring. Furthermore, conjugated carbonyl functionality at $\delta_C$ 181.3 (C-4″) in the molecule was identified by an analysis of $^{13}$C NMR spectrum (Table 1). The HMBC spectrum showed that H-3″ and H-6″ correlated with C-4″, indicating that one of proposed aryl groups is actually a cyclohexadienone group.[14] In addition to aromatic signals, the $^1$H NMR spectrum exhibited five sp$^3$ methines, one sp$^3$ methylenes, three methyls, and eight methoxy groups. The $^{13}$C NMR spectrum of **2** showed 35 carbon resonances corresponding to the above protonated units and 12 quaternary carbons. The protonated carbons and their bonded protons were assigned unambiguously by the HSQC data. The detailed interpretation of the $^1$H−$^1$H COSY spectrum led to the identification of one isolated proton spin-system corresponding to the C7−C8(C9)−C7′−C8′(C9′)−C7″−C8″−C9″ subunit of **2**. The HMBC spectrum was used to confirm the above proton spin-system assignment and establish the connectivities among the fractions. HMBC correlations of H-8 and H-8′ with C-1″ established a cyclohexane moiety; in turn, correlations from H-3″ and H-6″ to C-1″, C-2″, C-4″, and C-5″ allowed the establishment of a spirodienone moiety. In addition, HMBC correlations from H-7 to C-1, C-2, and C-6 established the connection of C-1 with C-7, and HMBC correlations of H-7′ with C-1′, C-2′, and C-6′ established the connection of C-1′ with C-7′. With the aid of 2D spectra, all the signals could be assigned unambiguously.

The relative configuration of **2**, as well as the conformation of the cyclohexane ring, were elucidated through coupling constants and the analysis of its NOESY spectrum. A large vicinal coupling constant (11.0 Hz) between H-7 and H-8 revealed a trans-diaxial relationship of H-7/H-8. The NOESY correlations of H-7/H-7′, H-7/H-7″, and H-7′/H-7″ indicated that these three protons were spatially arranged on the top face of the molecule as axial protons, whereas H-8 showed a strong NOE correlation with $H_3$-9′, indicating that these two protons were in axial protons on the bottom face of the molecule. As expected, correlations from H-7 and H-7′ to H-8 and from H-7′ and H-7″ to $H_3$-9′ were not observed. The remaining groups (H-8′, $H_3$-9, ethyl group, as well as two tetrasustituted aromatic ring groups) were therefore assigned equatorial positions. Furthermore, H-6″ showed correlations with H-8 and $H_3$-9′, which indicated that the dienone ring was oriented perpendicularly to the cyclohexane ring.

In the NOESY spectrum, H-7 also exhibited a strong NOE correlation with H-6, whereas the NOE correlations of H-8 and H-6″ with H-6 were not observed, revealing that H-6 was spatially close to H-7. These data suggested that the great steric hindrance between benzene ring A at C-7 and the dienone ring prevented the interconversion of benzene ring A, thus allowing the adoption of only one conformer to form a stable atropisomer at room temperature. In addition, H-8 and $H_3$-9′ showed strong NOE correlations with H-6′, while the NOE correlation of H-7′ with H-6′ was not observed, suggesting that H-6 was spatially close to both H-8 and $H_3$-9′. These data suggested that the rotation between C-1′ and C-7′, at room temperature, was


dx.doi.org/10.1021/jo1022712 |J. Org. Chem. 2011, 76, 2056–2061

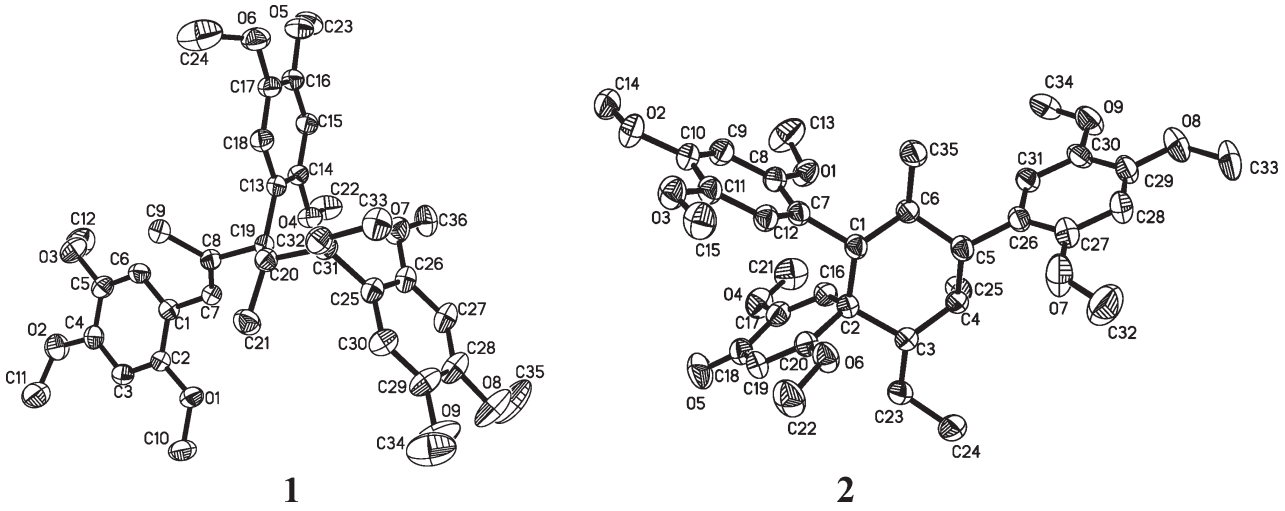


**Figure 3.** X-ray crystallographic structures of **1** and **2**.

restricted due to the methyl group at C-9. A X-ray crystallographic analysis (Figure 3) was successfully conducted to confirm the relative configuration of **2**, which was in good accordance with that of the solution structure **2** as established by the NOESY spectrum.

Tatanan C (**3**) has the same molecular formula as **2**. It gave spectroscopic data very similar to those of **2** (Table 1). However, resonances for H-7 and H-8 of **3** were significantly shifted, respectively, by $\Delta\delta_H$ +0.67 and −0.64 ppm, when compared with those of **2**. In addition, C-7 of **3** was significantly shielded by $\Delta\delta_C$ −10.4 ppm, whereas C-8 of **3** was deshielded by $\Delta\delta_C$ +2.9 ppm. Accordingly, it might be proposed that **3** was an atropisomer of **2**. This was confirmed by its 2D NMR data, the NOE difference experiments, and coupling constants. In the NOE difference experiments, H-8 and H-6″ of **3** were enhanced by irradiation of H-6, whereas H-7 was not enhanced, revealing that H-6 was spatially close to both H-8 and H-6″. The rest of the relative configuration of **3** was determined to be the same as that of **2** from further analysis of the NOESY spectrum (Figure 2). Therefore, **3** was assigned as an atropisomer possessing the relative configuration illustrated in Figure 2. After the solution of **2** was stood at room temperature for three months, we observed that about 10% of **2** converted into **3** (Figure S49 in the Supporting Information). The $^1$H NMR spectra from a NMR temperature experiment on the mixture of **2** and **3** showed that the signals of **3** increased from 45% at 20 °C to 50% at 80 °C (Figure S50 in the Supporting Information). A variable-temperature $^1$H NMR experiment from 30 to 80 °C was also conducted on compound **3**, whereas the $^1$H NMR spectra showed that the inversion of A-ring did not occur (Figure S51 in the Supporting Information). This substantiates the high energy barrier between **2** and **3**.

The content of **1** in the $CH_2Cl_2$ extract of rhizomes of *A. tatarinowii* was determined. Quantitative analysis was performed by an HPLC−DAD method with the above isolated sample as external standards. In the $CH_2Cl_2$ extract of rhizomes, **1** constituted (7.80 ± 0.58) $\mu$g mg$^{-1}$. This method also provides a simple and fast approach to identify and separate **1** from the rhizomes of *A. tatarinowii*, which is important to developing the pharmaceutical potential of tatanans.

Tatanans A−C were evaluated for their in vitro antidiabetic activities, including GK activity, dipeptidyl-peptidase-4 (DPP-4) antagonist activity, α-glycosidase inhibitory activity, $Na^+$-glucose cotransporter (SGLT) antagonist activity, and aldose reductase inhibitory activity. These novel metabolites displayed potent and selective in vitro GK activity with **3** being the most active congener observed in this study, as shown in Table 2. Their activities were more potent than that of GKA22,[15] one of the most potent GK activators reported in vitro to date, serving as a positive control. In addition, all metabolites were inactive against DPP-4, α-glycosidase, SGLT, and aldose reductase (Tables S1−4 in the Supporting Information).

**Table 2. In Vitro Activation of GK by Tatanans A−C (1−3)**

| compd | $EC_{1.5}$[a] ($\mu$M) | GK fold activation at 10 $\mu$M |
|---|---|---|
| **1** | 1.85 | 1.9 |
| **2** | 0.52 | 2.2 |
| **3** | 0.16 | 2.2 |
| GKA22 | 3.01 | 1.7 |

[a] Potency was measured as the concentration of compound required to increase enzyme activity by 50%.

## CONCLUSIONS

In summary, our results are encouraging and might be a promising basis for the development of a novel class of antihyperglycemic agents. Tatanan A was proved to be optically pure by chiral HPLC analysis. This implies that the biosynthesis of tatanan A is under strict enantioselective control of monomer coupling. However, single crystals of tatanan B had space group $P2_1/n$, indicative of its racemic nature that was also supported by its lack of optical activity. Tatanan C is also racemic, as evidenced by its lack of optical activity. Though many types of lignans with an enormous structural diversity have been isolated from plants of more than seventy families,[16] this is first report of C8−C7′ linked sesquinlignan. To the best of our knowledge, no other structure with this skeleton has been reported to date. Tatanans B and C were atropisomers with hindered rotation around the C-1−C-7 bond. Structurally, they possess an unprecedented spiro[5.5]undeca skeleton, with two benzyl moieties attached to C-7 and C-7′ respectively. Considering the structural novelty and potent GK activity, the biosynthesis of tatanans are worthy of further attention.


dx.doi.org/10.1021/jo1022712 |*J. Org. Chem.* 2011, 76, 2056–2061

## EXPERIMENTAL SECTION

**Collection, Extraction, and Isolation Procedures.** The rhizomes of *A. tatarinowii* were purchased from a Chinese herb store in Anguo country, Hebei Province, China, and authenticated by Professor Lin Ma, Institute of Materia Medica, Chinese Academy of Medical Sciences and Peking Union Medical College. A voucher specimen (No. S-2286) has been deposited at the Herbarium of the Institute of Material Medica, Chinese Academy of Medical Sciences and Peking Union Medical College, China. The air-dried powder of the rhizomes of *A. tatarinowii* (18 kg) was extracted with 95% EtOH under reflux (each time 1 h, 5 L × 3 times). All of the extracts were combined and concentrated under vacuum to give a residue (1.9 kg), which was suspended in water and extracted with petroleum ether (1 L × 3), ethyl acetate (1 L × 3), and *n*-butanol (1 L × 3) successively. The organic solvents were evaporated under reduced pressure to provide extracts of petroleum ether (360 g), ethyl acetate (400 g), and *n*-butanol (320 g). The EtOAc-soluble fraction (400 g) was subjected to silica gel chromatography ($CHCl_3$/MeOH, from 100/0 to 0/100, v/v) to give 20 fractions (Fr.A−Fr.T). Fraction E (40 g) was repeatedly subjected to silica gel chromatography eluted with PE−acetone (10:1−8:1−6:1−4:1−2:1−1:1, v/v) to provide nine subfractions ($Fr.E_1$−$Fr.E_9$). Subfraction $Fr.E_7$ (3.5 g) was submitted to RP-MPLC (MeOH−$H_2O$, 50:50 to 100:0), yielding $Fr.E_{71}$−$Fr.E_{79}$. $Fr.E_{76}$ (320 mg)was submitted to silica gel chromatography eluted with PE−EtOAc to yield $Fr.E_{761}$−$Fr.E_{765}$. $Fr.E_{763}$ (70 mg) was purified by HPLC (MeOH−$H_2O$, 80:20) to yield **1** (30 mg). Subfraction $Fr.E_8$ (2.1 g) was submitted to RP-MPLC (MeOH−$H_2O$, 50:50 to 100:0), yielding $Fr.E_{81}$−$Fr.E_{89}$. $Fr.E_{85}$ (170 mg) was submitted to silica gel chromatography eluted with PE−EtOAc to yield $Fr.E_{851}$−$Fr.E_{854}$. $Fr.E_{853}$ (65 mg) was purified by RP-HPLC (MeCN−$H_2O$, 60:40) to yield **2** (12 mg) and **3** (10 mg).

**Quantification of Tatanan A (1) in the $CH_2Cl_2$ Extract.** The rhizomes of *A. tatarinowii* (50 g) were powdered and then extracted with $CH_2Cl_2$ in an ultrasonic bath at temperature of 25 °C for 30 min. The extract was concentrated under vacuum at room temperature to give a residue (25 mg). Compound **1** in the residue was identified by comparison of its UV spectrum, and retention time with those of the authenticated compound available in the laboratory. Subsequently, compound **1** in the residue was collected by preparative HPLC according to its retention time and then was analyzed by HPLC−HRESI−MS (Figures S2 and S3 in the Supporting Information).

An isocratic system of mobile phase comprising a mixture of methanol/water was used with a flow rate of 1 mL/min. The injection volume of samples was 20 $\mu$L. The compounds were detected at 254 nm, and their retention times, peak areas and UV spectra were compared with those of authentic compounds. Calibration curve for compound **1** was prepared. Triplicate injections were made at five concentrations (10, 20, 50, 100, and 200 $\mu$g/mL). The linearity of each standard curve was made by plotting the peak areas versus concentration. The equation and correlation coefficient obtained from the linearity studies was $y = 0.00005x - 0.6266$ ($R^2 = 0.9995$) for **1**.

**In Vitro Glucokinase Enzymatic Assays.** GK activity was measured in a coupled reaction with glucose-6-phosphate dehydrogenase (G6PDH) by monitoring nicotinamide adenine dinucleotide phosphate (NADPH) production by the increase rate of absorbance at 340 nm. Briefly, GK was incubated with DMSO solution in assay buffer containing 100 mM Tris-HCl, pH 7.4, 25 mM ATP, 1 mM NAD, 5 mM DTT, 2 mM $MgCl_2$, 25 mM KCl, 4 mM glucose, 4.5 mU G6PDH, and 2 mU GK at 30 °C. The OD values were measured at each concentration of the compound, using the OD value of the DMSO control as 100%. The $EC_{1.5}$ ($\mu$M) values were calculated from the OD value at each concentration. The velocities of the enzyme reaction were expressed as mOD/min, and the fold activation of the enzyme was achieved by comparing with control.

**Spectral data of tatanan A (1):** white solid, crystallized from MeOH; mp 125−127 °C; $[\alpha]^{20}_D$ +10 ($c$ = 0.1, MeOH); UV (MeOH) $\lambda_{max}$ nm (log $\varepsilon$) = 204 (4.94), 232 (sh, 4.45), 259 (4.21) and 296 (4.32); IR $\nu_{max}$ 2968, 2934, 2885, 2845, 1606, 1509, 1465, 1454, 1205, 1036 $cm^{-1}$; $^1H$ NMR ($CD_3OD$, 500 MHz) and $^{13}C$ NMR ($CD_3OD$, 125 MHz) see Table 1; HREIMS $m/z$ 624.3267 $[M]^+$, calcd for $C_{36}H_{48}O_9$, 624.3298.

**Spectral data of tatanan B (2):** white needles, mp 216−218 °C; $[\alpha]^{20}_D$ 0 ($c$ = 0.1, MeOH); UV (MeOH) $\lambda_{max}$ nm (log $\varepsilon$) = 203 (5.08), 232 (4.44), 258 (4.39) and 289 (4.26); IR $\nu_{max}$ 2961, 2935, 2836, 1655, 1635, 1598, 1513, 1460, 1208, 1034 $cm^{-1}$; $^1H$ NMR (acetone-$d_6$, 500 MHz) and $^{13}C$ NMR (acetone-$d_6$, 125 MHz) see Table 1; HREIMS $m/z$ 610.3143 $[M]^+$, calcd for $C_{35}H_{46}O_9$ 610.3142.

**Spectral data of tatanan C (3):** white needles, 166−168 °C; $[\alpha]^{20}_D$ 0 ($c$ = 0.11, MeOH); UV (MeOH) $\lambda_{max}$ nm (log $\varepsilon$) = 205 (5.01), 230 (4.39), 260 (4.32) and 289 (4.18); IR $\nu_{max}$ 2962, 2933, 2834, 1651, 1632, 1594, 1510, 1454, 1206, 1032 $cm^{-1}$; $^1H$ NMR ($CD_3OD$, 500 MHz) $\delta$ 0.43 (d, $J$ = 6.0 Hz, H-9), 0.74 (t, $J$ = 7.0 Hz, H-9″), 0.88 (d, $J$ = 7.5 Hz, H-9′), 1.02 (m, H-8″a), 1.21 (m, H-8″b), 2.27 (m, H-8′), 2.47 (dt, $J$ = 11.0, 4.5 Hz, H-7″), 2.60 (m, H-8), 3.30 (dd, $J$ = 11.5, 4.5 Hz, H-7′), 3.78 (d, $J$ = 11.5 Hz, H-7), 3.64, 3.68, 3.71, 3.72, 3.75, 3.76, 3.80 (OMe × 8), 5.29 (s, H-3″), 6.26 (s, H-6″), 6.42 (s, H-3), 6.64 (s, H-3′), 6.69 (s, H-6), 6.92 (s, H-6′). $^{13}C$ NMR ($CD_3OD$, 125 MHz) $\delta$ 121.0 (C-1), 153.8 (C-2), 98.0 (C-3), 150.0 (C-4), 143.0 (C-5), 117.3 (C-6), 51.7 (C-7), 30.7 (C-8), 18.9 (C-9), 124.6 (C-1′), 154.2 (C-2′), 99.6 (C-3′), 149.7 (C-4′), 144.0 (C-5′), 117.2 (C-6′), 48.7 (C-7′), 33.8 (C-8′), 12.4 (C-9′), 56.6 (C-1″), 182.8 (C-2″), 104.1 (C-3″), 184.4 (C-4″), 152.5(C-5″), 117.0(C-6″), 50.0(C-7″), 22.5(C-8″), 12.0(C-9″), 55.0, 56.0, 56.1, 56.3, 56.5, 56.8, 57.8, 58.4 (OMe × 8); $^1H$ NMR (acetone-$d_6$, 600 MHz) and $^{13}C$ NMR (acetone-$d_6$, 150 MHz) see Table 1. HREIMS $m/z$ 610.3128 $[M]^+$, calcd for $C_{35}H_{46}O_9$, 610.3142.

**X-ray Crystal Data for Tatanan A (1).** $C_{36}H_{48}O_9$, $M$ = 624.77, monolicinic, space group $P2_1$, $a$ = 10.969(7) Å, $b$ = 8.042(8) Å, $c$ = 19.434(12) Å, $V$ = 1706.7(1)Å$^3$, $Z$ = 2, $d$ = 1.215 g/cm$^3$. Final indices were $R_1$ = 0.0556, w$R_2$ = 0.1565 ($w = 1/\sigma|F|^2$), $S$ = 1.047. Cu Kα radiation. A single crystal of dimensions 0.10 × 0.10 × 0.20 mm was used for X-ray measurements. The total number of independent reflections measured was 4163, of which 4085 were observed ($|F|^2 \geq 2\sigma|F|^2$). The crystal structure of **1** was solved by direct methods and refined with full-matrix least-squares calculations on $F^2$. The absolute structure was determined giving a Flack parameter of 0.0(3). The CIF file of X-ray data of **1** has been deposited in the Cambridge Crystallographic Data Centre (deposition no.: CCDC 772121).

**X-ray Crystal Data for Tatanan B (2).** $C_{35}H_{46}O_9$, $M$ = 610.74, monolicinic, space group $P2_1/n$, $a$ = 8.792(1) Å, $b$ = 15.306(1) Å, $c$ = 24.545(1) Å, $V$ = 3279.0(5) Å$^3$, $Z$ = 4, $d$ = 1.237 g/cm$^3$. Final indices were $R_1$ = 0.0938, w$R_2$ = 0.1355, $S$ = 1.026. Cu Kα radiation. A single crystal of dimensions 0.20 × 0.20 × 0.20 mm was used for X-ray measurements. The total number of independent reflections measured was 5979, of which 4470 were observed ($|F|^2 \geq 2\sigma|F|^2$). The crystal structure of **2** was solved by direct methods and refined with full-matrix least-squares calculations on $F^2$. The CIF file of X-ray data of **2** has been deposited in the Cambridge Crystallographic Data Centre (deposition no.: CCDC 772122).

## ASSOCIATED CONTENT

**Supporting Information.** UV, IR, MS, and NMR spectra for compounds **1**−**3**; flowchart for the isolation procedure, biological data about dipeptidyl-peptidase-4 (DPP-4) antagonist activity, α-glycosidase inhibitory activity, $Na^+$−glucose cotransporter (SGLT) antagonist activity, and aldose reductase inhibitory activity, and liquid chromatogram of the $CH_2Cl_2$ extract of

*A. tatarinowii*. This material is available free of charge via the Internet at http://pubs.acs.org.

## AUTHOR INFORMATION

**Corresponding Author**

*To whom correspondence should be addressed. Tel: +86-10-63165224. Fax: +86-10-63017757. E-mail: dqyu@imm.ac.cn.

## ACKNOWLEDGMENT

This research was supported by National Science and Technology Project of China (No. 2009ZX09311-004) and the Key Laboratory of Bioactive Substances and Resources Utilization of Chinese Herbal Medicine, Peking Union Medical College, Ministry of Education.

## REFERENCES

(1) Wild, S.; Roglic, G.; Green, A.; Sicree, R.; King, H. *Diabetes Care* **2004**, *27*, 1047–1053.
(2) Saltiel, A. R.; Kahn, C. R. *Nature* **2001**, *14*, 799–806.
(3) Gershell, L. *Nat. Rev. Drug Discov.* **2005**, *4*, 367–368.
(4) Matschinsky, F. M.; Glaser, B.; Magnuson, M. A. *Diabetes* **1998**, *47*, 307.
(5) Grimsby, J.; Sarabu, R.; Corbett, W. L.; Haynes, N.-E.; Bizzarro, F. T.; Coffey, J. W.; Guertin, K. R.; Hilliard, D. W.; Kester, R. F.; Mahaney, P. E.; Marcus, L.; Qi, L.; Spence, C. L.; Tengi, J.; Magnuson, M. A.; Chu, C. A.; Dvorozniak, M. T.; Matschinsky, F. M.; Grippo, J. F. *Science* **2003**, *301*, 370–373.
(6) Matschinsky, F. M. *Nat. Rev. Drug Discov.* **2009**, *8*, 399–416.
(7) Sarabu, R.; Berthel, S. J.; Kester, R. F.; Tilley, J. W. *Exp. Opin. Ther. Patents* **2008**, *18*, 759.
(8) Daniewski, A. R.; Liu, W.; Radinov, R. N. WO Patent 2007/115968 .
(9) Bertram, L. S.; Black, D.; Briner, P. H.; Chatfield, R.; Cooke, A.; Fyfe, M. C. T.; Murray, P. J.; Naud, F.; Nawano, M.; Procter, M. J.; Rakipovski, G.; Rasamison, C. M.; Reynet, C.; Schofield, K. L.; Shah, V. K.; Spindler, F.; Taylor, A.; Turton, R.; Williams, G. M.; Wong-Kai-In, P.; Yasuda, K. *J. Med. Chem.* **2008**, *51*, 4340–4345.
(10) Liao, W. P.; Chen, L.; Yi, Y. H.; Sun, W. W.; Gao, M. M.; Su, T.; Yang, S. Q. *Epilepsia* **2005**, *46*, 21–24.
(11) Hu, J. F.; Feng, X. Z. *Planta Med.* **2000**, *66*, 662–664.
(12) Cesspooch, L. *Native American Traditional Medicine and Diabetes*, 2005, http://hlunix.hl.state.ut.us/diabetes/telehealth/2005archives.htm.
(13) Si, M. M.; Lou, J. S.; Zhou, C. X.; Shen, J. N.; Wu, H. H.; Yang, B.; He, Q. J. *J. Ethnopharmacol.* **2010**, *128*, 154–159.
(14) Sinkkonen, J.; Liimatainen, J.; Karonen, M.; Wiinamäki, K.; Eklund, P.; Sjöholm, R.; Pihlaja, K. *Angew. Chem., Int. Ed.* **2007**, *46*, 4148–4150.
(15) Mckerrecher, D.; Allen, J. V.; Bowker, S. S.; Boyd, S.; Caulkett, P. W. R.; Currie, G. S.; Davies, C. D.; Fenwick, M. L.; Gaskin, H.; Grange, E.; Hargreaves, R. B.; Hayter, B. R.; James, R.; Johnson, K. M.; Johnstone, C.; Jones, C. D.; Lackie, S.; Rayner, J. W.; Walker, R. P. *Bioorg. Med. Chem. Lett.* **2005**, *15*, 2103–2106.
(16) (a) Whiting, D. A. *Nat. Prod. Rep.* **1985**, *2*, 191–211. (b) Pan, J. Y.; Chen, S. L.; Yang, M. H.; Wu, J.; Sinkkonen, J.; Zou, K. *Nat. Prod. Rep.* **2009**, *26*, 1251–1292.